

Supplementary Materials for

Thermoelastic properties of monolayer covalent organic frameworks studied by machine-learning molecular dynamics

Bing Wang, Penghua Ying[†], Jin Zhang^{*}

^aSchool of Science, Harbin Institute of Technology, Shenzhen 518055, PR China

^{*}Corresponding author. E-mail address: jinzhang@hit.edu.cn (J. Zhang).

[†]The present address: Department of Physical Chemistry, School of Chemistry, Tel Aviv University, Tel Aviv, 6997801, Israel

1. Supplementary figures

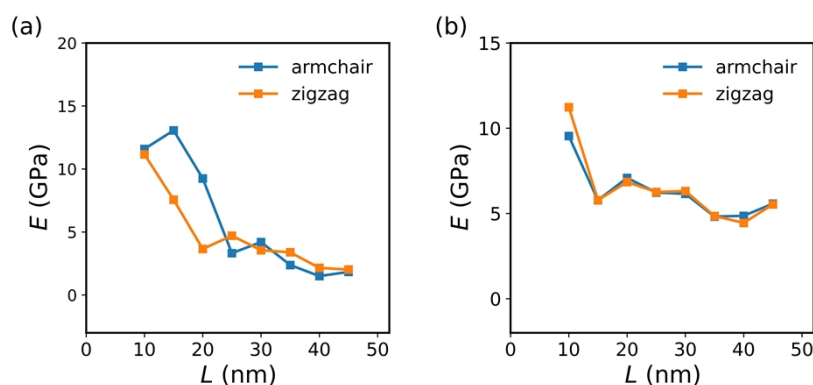


Fig. S1. The Young's moduli E of (a) COF-1 and (b) COF-5 monolayers at the room temperature and with different lengths L .

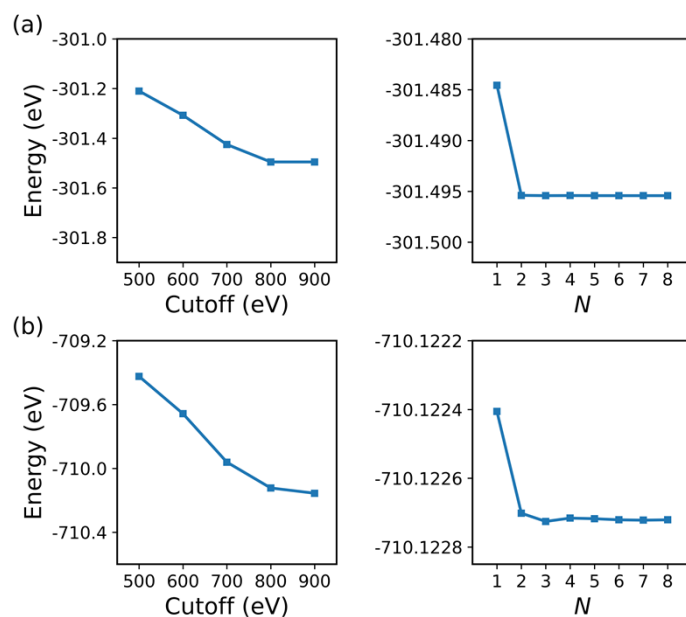


Fig. S2. The associated energy variation in (a) COF-1 and (b) COF-5 during the change of the energy cutoff and k-point grid dimension ($N \times N \times 1$) in DFT calculations.

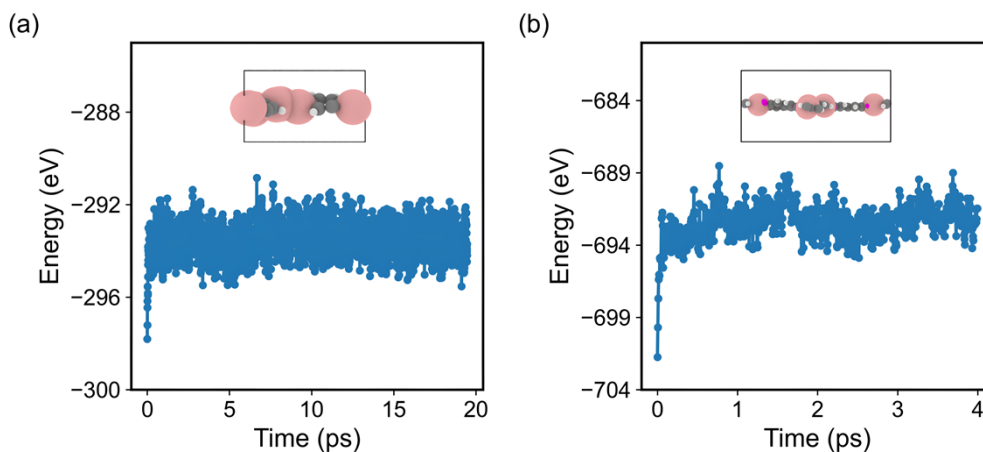


Fig. S3. Energy evolution of (a) COF-1 and (b) COF-5 during AIMD simulations at the temperature of 500 K.

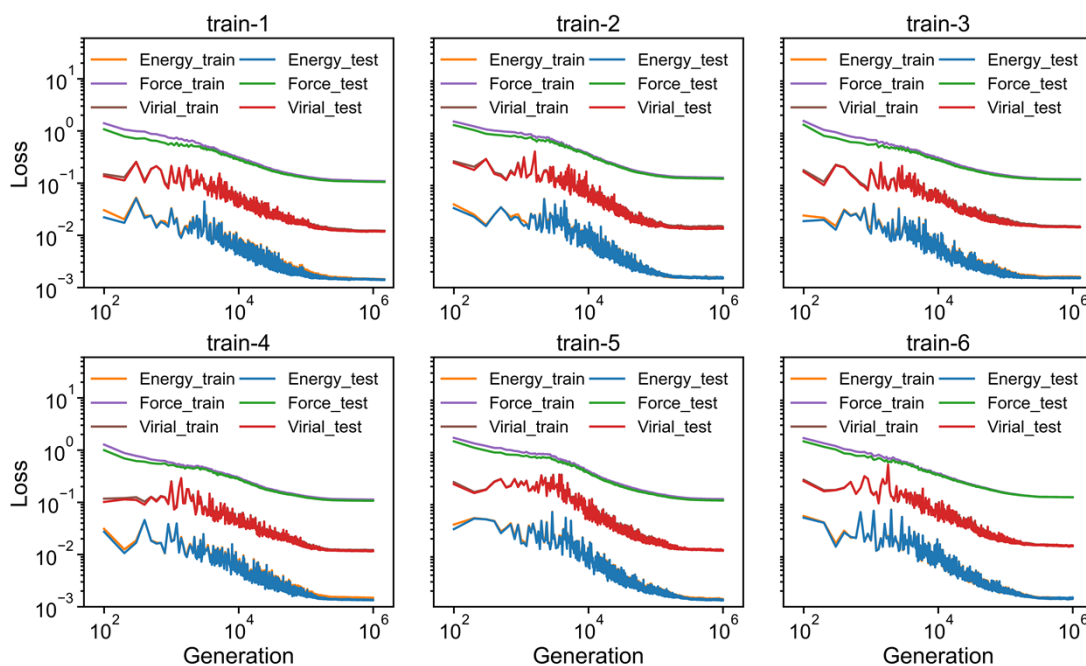


Fig. S4. The evolution of various loss functions for the training and testing dataset with respect to the generation of 2D COFs under different hyperparameters in Table S1. The RMSE for the training set is listed in Table S1.

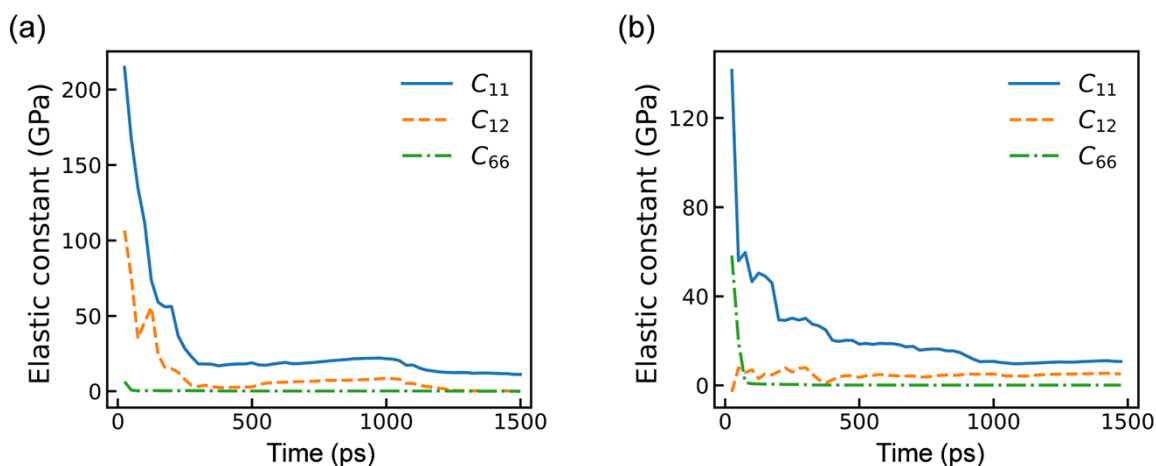


Fig. S5. Evaluation of elastic constants (C_{11} , C_{12} and C_{66}) with respect to simulation time at the temperatures of 100 K

for (a) COF-1 and (b) COF-5.

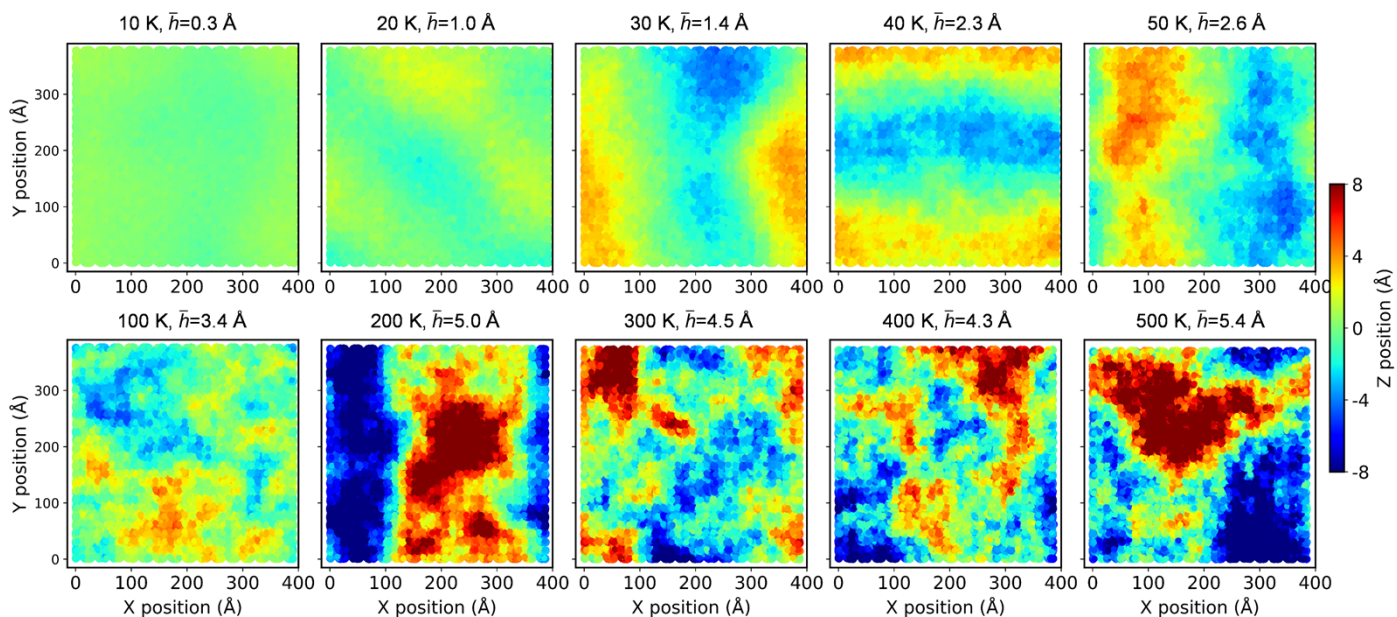


Fig. S6. Configurations of COF-1 at different temperatures. Here, contours illustrate the out-of-plane deformation of monolayer COFs.

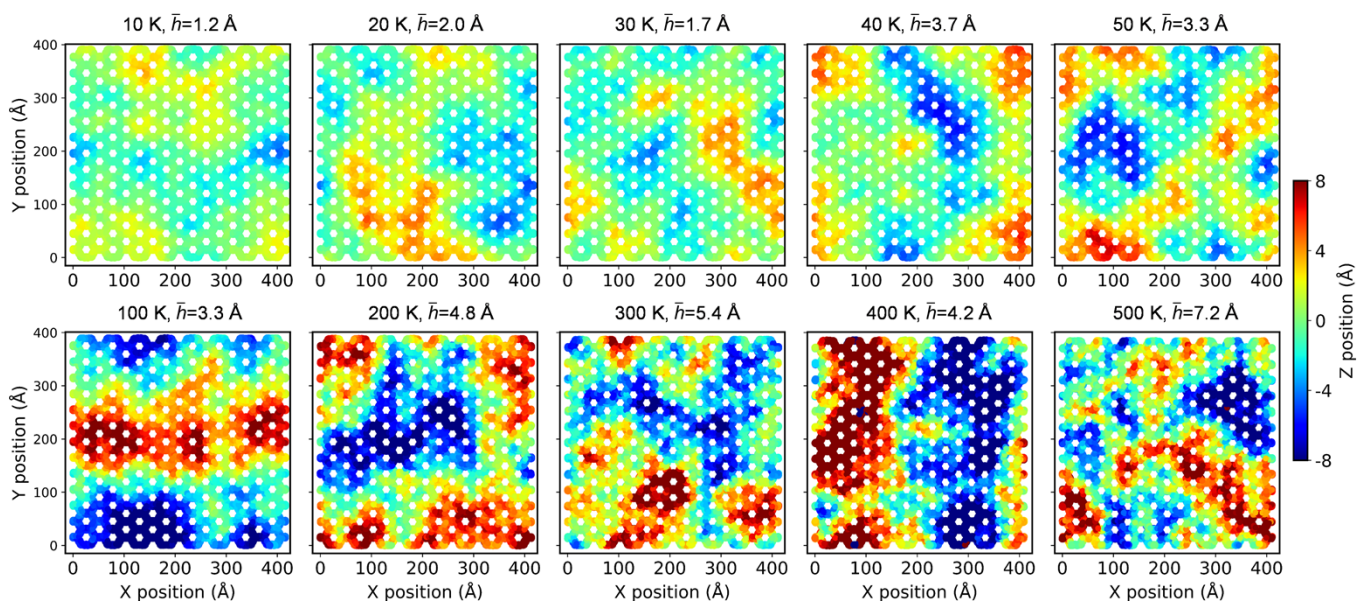


Fig. S7. Configurations of COF-5 at different temperatures. Here, contours illustrate the out-of-plane deformation of monolayer COFs.

2. Supplementary tables

Table S1. Hyperparameters of the NEP model used for training. Here, r_c^R represents the radial cutoff, r_c^A represents the angular cutoff, n_{\max}^R and n_{\max}^A , respectively, represent the Chebyshev polynomial expansion order for the radial and angular descriptor components. RMSE represents the energy, force and virial root mean squared error for the training set.

| Set number | Cutoff | | n_{\max} | | RMSE | | |
|------------|----------------|----------------|--------------|--------------|------------------|----------------------|----------------------|
| | r_c^R (Å) | r_c^A (Å) | n_{\max}^R | n_{\max}^A | Force (meV/Å) | Energy (meV/atom) | Virial (meV/atom) |
| 1 | 8 | 4 | 8 | 4 | 105.3 | 1.4 | 11.8 |
| 2 | 8 | 6 | 6 | 4 | 121.4 | 1.5 | 13.4 |
| 3 | 8 | 4 | 4 | 4 | 116.5 | 1.5 | 14.3 |
| 4 | 10 | 4 | 6 | 4 | 106.7 | 1.3 | 11.6 |
| 5 | 10 | 6 | 8 | 6 | 108.4 | 1.3 | 12.1 |
| 6 | 10 | 6 | 8 | 4 | 124.9 | 1.5 | 14.4 |

Table S2. A comparison among the Young's moduli of monolayer COF-5 extracted from present DFT calculations, NEP-based MD simulations, and previous MD simulations based on OPLS-AA force field.^{S1} Here, E_{zigzag} and E_{armchair} represent the Young's modulus in zigzag and armchair directions, respectively.

| Method | E_{zigzag} (GPa) | E_{armchair} (GPa) |
|---------------|---------------------------|-----------------------------|
| DFT (0 K) | 15.5 | 15.3 |
| NEP (0 K) | 15.1 | 14.9 |
| OPLS-AA (1 K) | 24.2 | 15.1 |

Reference

S1. H. Li and J.-L. Brédas, *Chem. Mater.*, 2021, **33**, 4529-4540.